



Missouri University of Science and Technology
Scholars' Mine

International Conferences on Recent Advances in Geotechnical Earthquake Engineering and Soil Dynamics 1995 - Third International Conference on Recent Advances in Geotechnical Earthquake Engineering & Soil Dynamics

05 Apr 1995, 4:00 pm - 4:20 pm

Numerical Modelling Approaches for the Analysis of Earthquake Triggered Landslides

H. Modaressi

Bureau de Recherches Géologiques et Minières, Orléans/ GRECO-Géomatériaux, France

D. Aubry

École Centrale de Paris, Châtenay-Malabry/ GRECO-Géomatériaux, France

E. Faccioli

Politecnico di Milano, Italy

C. Noret

Coyne et Bellier, France

Follow this and additional works at: <https://scholarsmine.mst.edu/icrageesd>

 Part of the [Geotechnical Engineering Commons](#)

Recommended Citation

Modaressi, H.; Aubry, D.; Faccioli, E.; and Noret, C., "Numerical Modelling Approaches for the Analysis of Earthquake Triggered Landslides" (1995). *International Conferences on Recent Advances in Geotechnical Earthquake Engineering and Soil Dynamics*. 3.

<https://scholarsmine.mst.edu/icrageesd/03icrageesd/session15/3>

This Article - Conference proceedings is brought to you for free and open access by Scholars' Mine. It has been accepted for inclusion in International Conferences on Recent Advances in Geotechnical Earthquake Engineering and Soil Dynamics by an authorized administrator of Scholars' Mine. This work is protected by U. S. Copyright Law. Unauthorized use including reproduction for redistribution requires the permission of the copyright holder. For more information, please contact scholarsmine@mst.edu.



Numerical Modelling Approaches for the Analysis of Earthquake Triggered Landslides

Paper No. INVLE.03

H. Modaressi

Research Division, Bureau de Recherches Géologiques et
Minières, Orléans, GRECO-Géomatériaux, France

D. Aubry

Ecole Centrale de Paris, Châtenay-Malabry, GRECO-
Géomatériaux, France

E. Faccioli

Politecnico di Milano, Milano, Italy

C. Noret

Coyne et Bellier, Gennevilliers, France

SYNOPSIS: Different numerical approaches for the analysis of earthquake triggered landslides are studied. Improved simplified models are developed and their performance for evaluating the response of natural slopes subjected to earthquakes is studied. Using more sophisticated numerical techniques the influence of several factors such as the hydromechanical behaviour assumptions, 1D vs. 2D geometry, and the input motion are assessed. 2D computations have shown that the kinematics of the slope motion is largely affected by the geometry of the slope. As far as the soil behaviour is concerned, the results indicate that introduction of progressive yielding in the soil model provides larger displacement, progressive pore-pressure generation and more diffuse deformation. For the input motion, the number of peaks and their amplitudes have been identified as being the main factors for irreversible displacements.

INTRODUCTION

This paper summarises part of the research work performed in the framework of the European research project "Analysis and Mitigation of Earthquake Triggered Landslide Hazard Affecting Dams, Routes and Lifelines". The prediction of earthquake triggered landslides along lifelines, dam reservoirs and inhabited zones is of great importance for many points of view. Among the motivations of this project is the severe damage caused by the failure of natural slopes during major recent earthquakes of the Mediterranean region, especially the Southern Italy (Irpinia) earthquake of 1980 that reactivated several pre-existing slides. Even though overconsolidated clays are common in earthquake prone areas of the Mediterranean and the focus of this paper is on the seismic response of natural cohesive soil slopes, some results for granular cohesionless soils are also presented.

Wilson and Keefer (1985) introduce the concept of critical displacement, i.e. the value beyond which a slope is likely to lose a significant amount of strength. For regional applications, they estimate it at 10 cm for coherent slides, but this value should depend on the sensitivity of infrastructures present in such a region.

Three successive stages (Ambraseys and Srbulov 1993) should be considered when investigating deformation caused by earthquakes in cohesive slopes. During the first, *co-seismic* stage, displacements tend to be small, and are controlled by the magnitude and duration of application of the earthquake inertia forces, by the geometry of the slope and, by the *undrained* strength of the material.

The second, *post-seismic* stage, will follow immediately after the earthquake if the "fast" residual undrained shear strength

on the slip surface is less than that required for maintaining static equilibrium. In this stage, displacements will be large if the reduction in strength is large, or if toe support is drastically reduced or lost, due to unfavourable topography or extreme loss of strength.

In the third stage, further movements may develop as a result of creep and consolidation processes, as well as from destabilizing hydrostatic forces if deep open cracks produced by the earthquake are filled with surface or ground-water. Such movements will be slow and associated with progressive failure and the drained strength of the soil.

Experimental evidence suggests that materials prone to rate-dependent behaviour, responsible for "second-stage" displacement, may be more common than expected and include OC clays, like those considered here.

Consideration of several key factors is necessary for a realistic analysis of natural slopes subjected to earthquakes: seismic input motion parameters (i.e. duration, frequency content, amplitude, number of peaks), vulnerability analyses (i.e. assessment of critical combination of predisposing and triggering factors), reliable models (i.e. geotechnical) and finally probabilistic or statistical approaches that may be sometimes sufficient for estimating the seismic motion.

In general the assessment of landslide vulnerability requires the application of criteria based on the interpretation of existing landslide systems for discriminating zones characterised by different levels of hazard. Criteria to be used for regional studies may consist of a simple overlay of different information, or may be based on models simulating the behaviour of slopes subjected to triggering events. These models can be either general sophisticated approaches including complex constitutive models and numerical

algorithms, or simplified models. The former permit multidimensional, non linear and multiphase analysis of soil slopes subjected to complex seismic wave patterns. Their application requires accurate field data which are unfortunately often sparse and incomplete. On the other hand, simplified methods provide a quick, approximate evaluation of the potential risk. However, standard methods as the pseudo-static method, which do not really take into account the dynamic aspect of the loading, and the standard Newmark method, are not appropriate for soil materials whose mechanical properties are affected by cyclic loading, especially when the soil is saturated (Tardieu *et al.* 1992). In the following section, some improved simplified models are proposed. They are at a balanced level between complexity of sophisticated methods and oversimplification of current simplified approaches.

SIMPLIFIED NUMERICAL MODELS

Slope failures consequent to seismic events are usually due to either an increase of active inertial forces of the soil mass or to a reduction of resistance caused by loss of strength. This resistance decrease in soils may be due to strain shearing and/or pore-pressure build-up induced by the earthquake cyclic loading. Therefore, the principal step for improving simplified models is to introduce such aspects of the soil behaviour in standard simplified models. Simple geometry is another feature of simplified methods. This aspect can be only partially improved (i.e. introduction of a 1D continuum approach instead of rigid block assumption). Another simplification consists in the use of a substitute short duration accelerogram instead of the real one. In such an input motion, the issue is to replace the natural accelerogram by a shorter earthquake characterised by the same response spectrum. The substitute accelerogram should be constructed by preserving the energy stored in the medium subjected to the real earthquake.

Improved Newmark Model (accounting for rate and pore pressure effects)

The starting point for simplified dynamic analysis is provided by the well known rigid block model (Newmark 1965). In addition to the geometry of the sliding mechanism, the main assumptions are that no loss in shear strength occurs during seismic loading and that the pore-pressure variations are negligible. Some improvements aimed at overcoming these restrictions are presented in the following subsections.

Rate effects

The influence of rate effects in cohesive soils are well-known in soil mechanics. A simplified model, accounting only for the dependence on displacement rate and not on displacement itself can be obtained by assuming a visco-plastic interface between rigid block and base. Then, the strength τ along the interface is a sum of a constant static residual strength τ_y and

a term depending on the displacement rate u :

$$\tau = \tau_y + \eta \dot{u} \quad (1)$$

where η is a viscosity type parameter.

With the previous assumptions, and expressing τ_y through the Mohr-Coulomb criterion, the equation of motion for the sliding block excited by the base acceleration $gk_h(t)$ is obtained:

$$\ddot{u} + \frac{\eta}{\rho} \dot{u} = g[k_h(t) - k_c] \frac{\cos(\theta - \phi)}{\cos \phi} \quad (2)$$

In the previous equation ρ denotes unit mass, g is the acceleration of gravity, θ the slope angle, ϕ the drained angle of shearing resistance and k_c the critical acceleration coefficient (Sarma 1979). The integration of previous equation gives an estimate of the permanent displacement induced by the earthquake.

In Fig. 1 an example is presented for a slope in London Clay subjected to the strong Tabas N16W earthquake. As it can be seen from the same figure, using the constant strength model would in this case result in an overestimation of final permanent displacement.

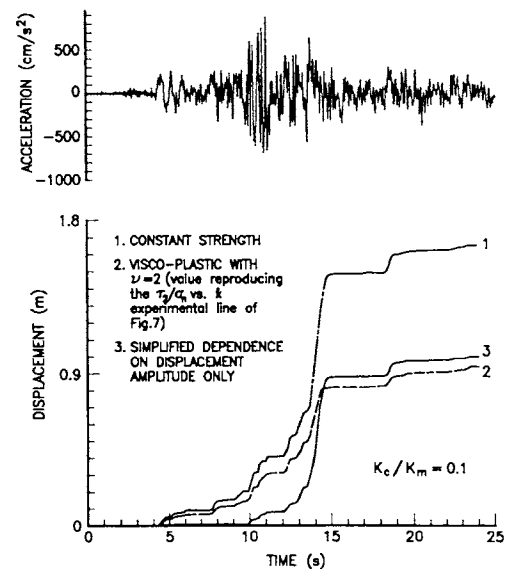


Fig. 1 - Displacement of rigid block to the Tabas 1978 acceleration (scaled at 0.87g, shown on the top).

Pore-pressure effects

Cyclic loading may result in pore-pressure generation in saturated soil, capable of affecting its strength along the sliding surface. A model has been developed by including both pore-water effects in undrained (short term) conditions and a more realistic relationship between the strength along the base and the relative displacement permitting progressive yielding (Aubry *et al.* 1990). In particular, a description based on the Cam-Clay model is used in order to prevent an indefinitely increasing dilatancy.

$$|\tau| = -\sigma' f(\sigma', \sigma_c) r([u_t]) \quad (3)$$

$$[\dot{u}_n] = -\left(\tan \psi + \frac{|\dot{\tau}|}{\sigma'} \right) \left| \frac{[\dot{u}_t]}{\sigma'} \right| \quad (4)$$

In the previous relationships, σ' is the normal stress, $[u_t]$ the tangential relative displacement, ϕ the friction angle and $\phi - \psi$ is a measure of the dilatancy on the sliding surface. The term $f(\sigma', \sigma_c)$, where σ_c is a critical state parameter of the soil, is introduced to prevent the irreversible normal relative displacement $[u_n]$ from increasing indefinitely on a dilatant sliding surface. The term $r([u_t])$ expresses the dependence of stress on tangential relative displacement with an assumed hyperbolic law:

$$r([u_t]) = \tan \phi \frac{[u_t]}{a + [u_t]} \quad (5)$$

The parameter a has a role of initial plastic modulus, its value being typically in the range of 10^{-5} - 10^{-3} . Upon unloading from a point $([u_t]_0, r_0)$ the previous expression is modified to:

$$r([u_t]) = r_0 + 2 \tan \phi \frac{[u_t] - [u_t]_0}{2a + |[u_t] - [u_t]_0|} \quad (6)$$

Since the analysis is carried out in undrained conditions, the total normal relative displacement is assumed to be constant, and this leads to the following relationship between the effective normal stress rate $\dot{\sigma}'$ and the rate of irreversible normal relative displacement $[\dot{u}_n]$:

$$\dot{\sigma}' = K [\dot{u}_n] \quad (7)$$

where K is an elastic normal stiffness coefficient. The above equation combined with overall equilibrium provides the variation of the pore water pressure in the form

$$\Delta p = -K [u_n] \quad (8)$$

The combination of the previous equations together with the equilibrium equation of the block determine the following expression for the critical acceleration coefficient:

$$k_c = \frac{(W \cos \theta - U) |q| - W j \sin \theta}{W [\cos \theta + j \sin \theta |q|]} \quad (9)$$

where with $q = \frac{\tau}{\sigma'}$, W is the weight of the block, and $j = 1$ if the block moves downward and -1 if it moves upward. U is the resultant of the water pressure acting on the base. The equation of motion of the block is written by imposing equilibrium both at limit conditions and during motion

(Chang *et al.* 1984), and has the form:

$$\ddot{u} = g \left[\frac{U |q| - U_c |q_c|}{W} + (k_h - k_c) \cos \theta - (|q| - |q_c|) \cos \theta + j (k_h |q| - k_c |q_c|) \sin \theta \right]$$

q_c and U_c being the values of q and U evaluated in conditions on incipient movement. For cohesive soils under rapid shearing it may be more appropriate to set $U = U_c$ and neglect Δp .

Alternative assumptions on Δp have been tested in the dynamic analysis of a cohesive slope, with $\phi = 10^\circ$, $a = 3.2E-5$, $K = 6.1E8$ Pa.m and $\theta = 4.5^\circ$. The latter is the inclination of the resultant static shear force along the slip surface. Results given in Fig. 2 indicate the strong sensitivity of the model to the parameter ψ . On the same figure, the opposite effects of the different assumptions on Δp should be noted.

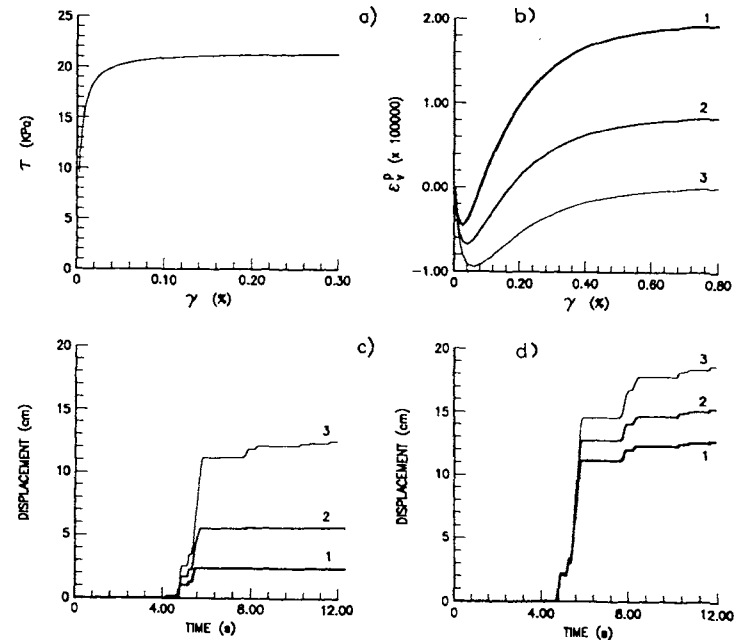


Fig. 2 - Stress-tangential relative displacement (a), normal vs. tangential relative displacements (b), displacement response of rigid block model to Sturmo accelerogram (c) and the same as (c) but with $\Delta p = 0$ assumption (d). Curves 1, 2 and 3 correspond to $\psi = 9^\circ$, 9.5° and 9.9° , respectively.

Extended 1D Model for deformable slope

A simplified model has been developed to simulate the behaviour of a slope subjected to seismic loading. It has been built up from the following considerations:

- oThe Slope is considered as two-dimensional and infinite in the steepest descent direction so that it is modelled by a 1D column perpendicular to the slope surface. It is located on a rigid bedrock, supposed to be parallel to the slope surface.
- oThe depth of the water table is assumed to be constant along the whole slope.

oThe true vertical component of accelerograms is neglected. The true horizontal component of the recorded earthquake is then projected in the direction of bedrock and in its orthogonal direction.

oPore water-soil interaction during loading is taken into account depending on the dilatancy/contractance characteristic of soil. This feature is of utmost importance in the case of saturated loose or medium sand, e.g. when liquefaction or a loss of shear resistance due to pore pressure increase is likely to occur.

For a given accelerogram, the model provides a diagnostic regarding the risk of liquefaction, and if liquefaction does not occur, the residual pore pressure and permanent downward displacement to be expected.

The seismic loading is modelled as a prescribed acceleration history of the rigid bedrock. Due to the symmetry of geometry, initial state and loading history, the problem appears to be purely one-dimensional, e.g. all points at a given depth have the same displacement, pore pressure, stress and strain histories. The displacement vector has two co-ordinates: the sliding in the slope direction, and the displacement normal to the slope surface. The related strain tensor reduces to the shear strain γ and the normal strain ε . The related stress tensor is characterised by the shear stress τ and the normal stress σ .

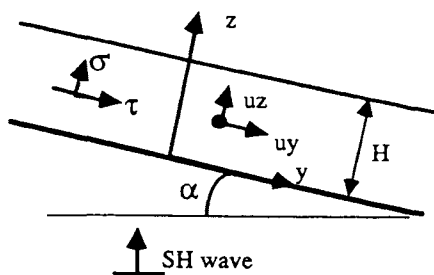


Fig.3 General layout of the model

The dynamic equations of the model in the absence of body forces are given as:

Drained case

$$\partial_z \tau = \rho(\partial_t v_y + a_{gy}) \quad (10)$$

$$\partial_z \sigma = \rho(\partial_t v_z + a_{gz})$$

Undrained case

$$\partial_z \tau = \rho(\partial_t v_y + a_{gy})$$

$$\sigma = \rho a_{gz}(t)(z - H) \quad (11)$$

$$p(z, t) = \rho a_{gz}(t)(z - H) - K \varepsilon^p$$

where ε^p is the plastic strain, K the elastic bulk modulus, σ the effective normal stress, p the pore pressure, H the depth of the soil slope, ρ the unit mass, v the velocity and a the prescribed input acceleration.

The final pore pressure when the seismic input motion is at

rest is thus given by:

$$p(z, T) = -K \varepsilon^p(z, T) \quad (12)$$

Although there is no dynamic settlement in this model a permanent static settlement will occur after the end of the seismic event ($t > T$) from the distribution of pore pressure under quasi static conditions.

Due to the symmetries assumed, the material's constitutive model can be reduced to a relationship relating the history of shear stress, effective normal stress and pore pressure to the history of shear and normal strain. Furthermore, it is assumed that the pore pressure is always nil above the water table (drained condition), whereas the evolution is supposed to be undrained below the water table. This assumption is correct in the case of very short term loading, such as earthquakes, and avoids solving the pore pressure diffusion equation. The proposed constitutive model is derived from the multi-mechanism cyclic Hujieux model, that has already been widely used in geotechnical applications: constitutive parameters are basically the same, and the same phenomena can be taken into account : elasticity, critical and characteristic state concepts, critical pressure, dilatancy/contractance, hardening/softening, cyclic hysteretic behaviour. However, some simplifications have been brought to the initial Hujieux model, and thus some parameters have been discarded. More precisely:

As in the Eq. (3), the plastic yield surface follows a hardening regime depending on the plastic shear strain γ^p and the influence of the critical stress σ_c is introduced as in the Cam-Clay model:

$$|\tau| = -\sigma' F r(\gamma^p) \quad (13)$$

with:

$$F(\sigma', \sigma_c(\varepsilon^p)) = 1 - b \ln(\sigma' / \sigma_c(\varepsilon^p)) \quad (14)$$

$$\sigma_c(\varepsilon^p) = \sigma_{c0} \exp(-\beta \varepsilon^p)$$

Where ϕ is the residual friction angle, b a shape parameter, β the volumetric hardening parameter and, σ_0 the initial critical pressure. It should be noted that in Eq. (3) the tangential relative displacement is used while in Eq. (13) the plastic shear strain is introduced. The original Hujieux hardening deviatoric rule has been adapted by replacing the parameter a (Eq. 5) with $\tan \phi / Ep$ and stiffening the hyperbolic hardening rule :

$$r(\gamma^p) = \tan \phi \left(\frac{\gamma^p}{\frac{\tan \phi}{Ep} + \gamma^p} \right)^n \quad (15)$$

where $n < 1$ is a non-dimensional parameter. Ep is the deviatoric hardening parameter. The previous equation is a generalised form of Eq. (5). Indeed, for $n = 1$, when simulating

a drained cyclic shear test, with an imposed cyclic strain amplitude, the variation of equivalent cyclic shear modulus G with γ could not be fitted with the typical $G(\gamma)$ curves; the transition from purely elastic behaviour (shear modulus = μ) to plastic behaviour (equivalent shear modulus $\#Ep\sigma$) is too sharp: a sudden drop of the curve appears when the strain becomes higher than the elastic strain.

The shape of the $G(\gamma)$ curve, as simulated for different values of n , other parameters remaining unchanged, is given on Fig. 4. On the same graph is also plotted a typical curve for soft clays, as given by Heiderbrecht *et al.* (1990). It can be seen that for $n=1/2$, the shape of the obtained curve is sufficiently smoothed and fits better the experimental one.

The evolution of the plastic strain rate is assumed to be given by a Roscoe type dilatancy rule:

$$\dot{\varepsilon}^p = -\zeta(\gamma^p) \left[\tan \psi + \frac{\tau}{\sigma'} \right] \left| \frac{\dot{\gamma}^p}{\gamma^p} \right| \quad (16)$$

with:

$$\zeta(\gamma^p) = 0, \text{ if } \gamma^p \leq \gamma^{pe}$$

$$\zeta(\gamma^p) = \left[(\gamma^p - \gamma^{pe}) / (\gamma^{pm} - \gamma^{pe}) \right]^{m_{cyc}}, \text{ if } \gamma^{pe} \leq \gamma^p \leq \gamma^{pm}$$

$$\zeta(\gamma^p) = 1, \text{ if } \gamma^p \geq \gamma^{pm}$$

where ψ is the angle defining the characteristic state and γ^{pe}, γ^{pm} are pseudo-elastic and mobilisation strains respectively. m_{cyc} is the parameter of the dilatancy mobilisation rule.

The equations are discretized with respect to the z variable by linear finite element and numerically integrated with respect to time by a Runge-Kutta scheme, with an adaptive time step.

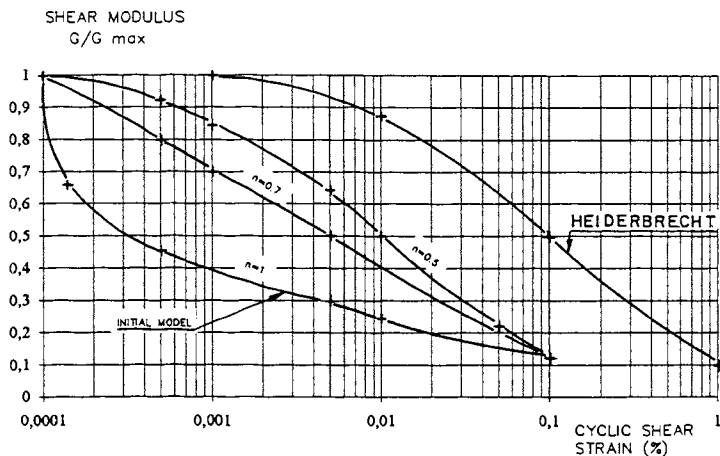


Fig. 4: Drained cyclic shear tests on Clays. $G(\gamma)$ curves for different values of n

The developed tool includes all the rheological concepts of the most sophisticated geotechnical finite element software, but it is easy and fast to run, because of the geometrical simplification. However, it has to be easy to use and efficient, even when very few in situ data are available.

For such cases, two "typical" sets of constitutive parameters

are proposed, one for clay and the other for sand. The variations of the parameters about these typical values are given, according to physical properties of the material (density, gradation, void ratio, plasticity index, ...). The determination of these parameters is described elsewhere (BRGM, 1989).

It has been checked that the proposed values are in agreement with most of the typical experimental data that are available in the literature, namely the curves relating the equivalent cyclic shear modulus to the cyclic shear deformation amplitude ($G(\gamma)$ curves) and the results of laboratory tests regarding sand liquefaction susceptibility (undrained shear box cyclic tests).

For clays, the elastic moduli G and K have been chosen according to the correlation proposed by Hardin. For a normally consolidated clay with a 5 meters overburden, $v_s=200$ m/s and $v_p=320$ m/s are selected. Actually, the variation of pore pressure under undrained condition is highly sensitive to the value of the bulk modulus.

The shape of the plastic yield surface in the normal stress/deviatoric stress plane is rounded, so that the value $b=1$ is usually chosen.

For highly plastic clays, the residual angle of shearing resistance is about 10° , whereas for very low plasticity clays, it is about 20° . A typical value $\phi=15^\circ$ can be given and $\psi < \phi$. $\psi < \phi$ results in a smaller contractant behaviour domain.

In the case of a normally consolidated clay, the stress state lies on the plastic yield surface and for $\phi=15^\circ$, $\sigma_0 \# 0.5 \sigma'$. According to the definition of the Over Consolidation Ratio (OCR), the initial critical pressure is about $\sigma_0 = \text{OCR} * \sigma' / 2$.

The β parameter is related to the slope Cc of the oedometric consolidation curve in the (void ratio, log of mean effective pressure) plot. The typical value for a medium clay is $\beta=10$. The maximum value for stiff clays (void ratio less than 0.45) is $\beta=20$, whereas for soft clays (void ratio more than 1) a typical value is $\beta=5$.

For clays, typical values of a are $10^{-4} < a < 10^{-3}$, which leads to $90 < Ep < 900$. With the values chosen for the other constitutive parameters, the value $Ep=700$ seems to be a mean value.

The value of all constitutive parameters are given in Table 1.

The shape of the yield surface in the (σ', τ) plane looks more like a straight line for sand. This corresponds to lower values of b . A typical value is $b=0.2$.

The residual friction angle mainly depends on the shape of the sand grains and on the mineralogy. It ranges from 25° to 40° . The value $\phi=35^\circ$ is chosen.

β is always higher than 30. It is about 100 for dense sands, about 60 for medium sands and 40 for loose sands.

Typical values of a are $10^{-3} < a < 10^{-2}$, which corresponds to $25 < Ep < 250$. The mean value $Ep=120$ is chosen.

The critical line and the characteristic line differ: the characteristic angle ψ is about 5° smaller than the friction angle ϕ . For $\phi=35^\circ$, the value $\psi=30^\circ$ is chosen.

In the case of sand, it has been considered that the parameter characterising the material's susceptibility to liquefaction is the initial critical pressure which has to be determined according to in situ data. Fig. 5 shows the influence of the

critical pressure on the variation of pore pressure during an undrained cyclic test.

For low values of the initial critical pressure, pore pressure increases strongly and the material comes to liquefaction, whereas for high values of the critical pressure, it develops cyclic mobility (slow increase of pore pressure).

Most of the liquefaction laboratory tests consist of undrained cyclic shear tests, with imposed shear stress. The results are generally given as the number of cycles leading to liquefaction or very high strains, for a given cyclic stress ratio, e.g. the ratio imposed cyclic shear stress/initial effective shear stress. A special numerical tool was thus developed to simulate such laboratory tests (driver with imposed shear stress conditions). By simulating such tests, one can plot the number N of cycles leading to failure of the sample, for different cyclic shear stress ratios, and for different values of the initial critical pressure.

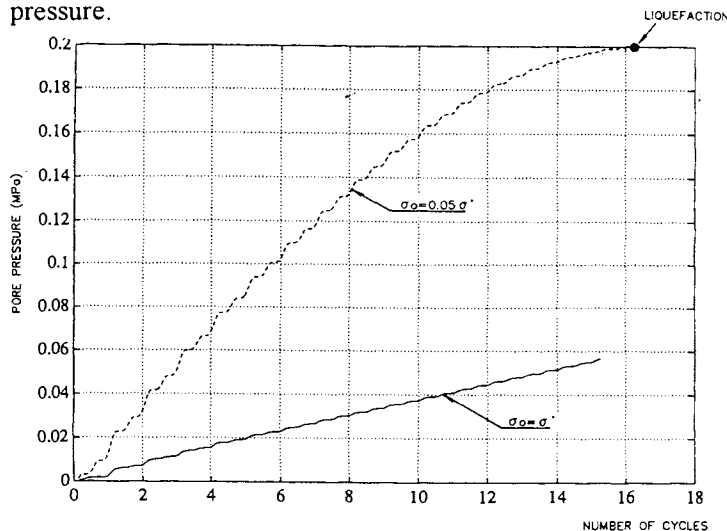


Fig. 5: Evolution of pore pressure during undrained simple shear test (imposed cyclic strain 10^{-3} , normal effective stress 0.2 MPa), for two values of the initial critical pressure.

parameter	sand	clay
shear modulus G	80 MPa	80 MPa
bulk modulus K	100 MPa	100 MPa
elastic strain γ_e	10^{-6}	10^{-5}
residual angle of shearing resistance ϕ	35°	15°
shape parameter b	0.2	1
initial critical pressure σ_0	according to liquefaction potential	$OCR \cdot \sigma' / 2$
volumetric hardening parameter β	60	10
deviatoric hardening parameter E_p	120	700
characteristic state angle ψ	30°	15°
pseudo-elastic radius r_e	0.025	0.072
mobilisation radius r_{pm}	0.56	0.21
mobilisation parameter m_{cyc}	2	2

Table 1 : Typical values for clay and sand

Parameters regarding dilatancy (ψ , γ_{pe} , γ_{pm} , m_{cyc}) and the bulk modulus K highly influence the variation of pore pressure.

As an example a slope is considered with a slope angle of 5° , and consisting of a 10 m sand layer. The water table is assumed to be located at a 5m. depth. The unit weight of the material is 2 t/m^3 .

The input signal imposed at the bedrock is a Tsang signal:

$$a(t) = A \cdot \alpha \cdot t \cdot \exp(-\alpha t) \cdot \sin(\omega t) \quad (17)$$

By changing values of A , ω and α , it is possible to change the frequency, amplitude and number of cycles of the signal. For the case study presented here, $\omega = 12.56 \text{ s}^{-1}$.

The model consists of two elements, including two nodes (plus the bedrock node) and two integration points. Displacements and accelerations are presented at both nodes and pore pressure and stress at the integration points, named "top" (actually at a 2.5 m. depth) and "mid-depth" (actually at a 7.5 m. depth).

Constitutive parameters for sand defined in the previous paragraph are chosen.

Different values of the PGA are tested, all other parameters remaining unchanged.

Fig. 6 gives the result of the analysis in the case of $PGA = 0.2g$ and, of an initial critical pressure of 0.2 MPa, about three times the initial effective normal stress. During the earthquake, the pore pressure tends successively to increase and decrease, as appears on the effective normal stress plot, which means that the stress state successively lies above and below the characteristic line, leading to successively contractant and dilatant behaviour. The maximum decrease of pore pressure is 0.05 MPa, which corresponds to negative pore pressure: the material actually would become unsaturated, which is not modelled here.

Due to the highly non-linear behaviour of the material, the amplification ratio is equal to 1 at mid-depth, which means that no amplification takes place, and the damping is very high.

As a conclusion, in the case of high initial critical pressure, due to the possible dilatancy of the material, the slope is likely to bear higher PGA without any tendency to liquefaction that could result in large permanent displacement. Smaller values of the initial critical pressure result in the liquefaction of the slope with the same amplitude of the input motion.

MORE GENERAL FINITE ELEMENT MODELS

Dynamic non-linear multidimensional finite element analyses for slopes may be performed for an accurate evaluation of displacement, stress and pore pressure. These computations have been rarely made for the assessment of natural slope stability, more often for geotechnical structures such as earthdams. The main difficulty arises from the lack of data on some major factors as initial stress state, seismic input motion and laboratory and *in situ* investigation for calibration of

constitutive models. A realistic numerical approach for dynamic slope failure analysis needs the use of techniques that are capable to capture the development of shear bands. These later progressively transform into sliding surfaces. The development of these techniques is a very active research domain in computational mechanics and still needs further investigations. However, in many slopes the evaluation of a critical displacement for a given structure, even before the sliding takes place, may be sufficient. In the present paper, we will be only concerned with such cases.

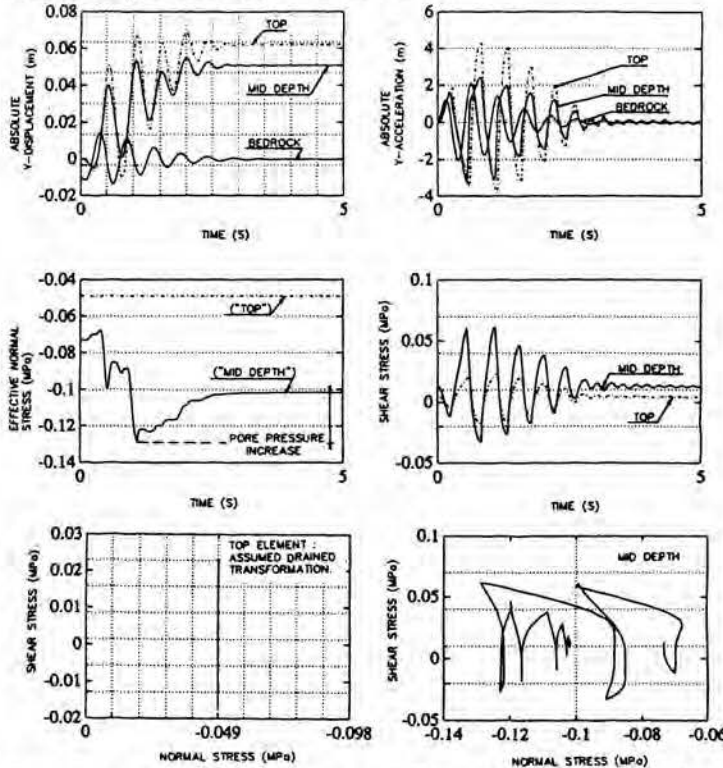


Fig. 6 : Input signal Tsang, PGA=0.2g, 4 cycles, critical pressure $\sigma_0=0.2$ MPa

In any case, different hypotheses with respect to geometry (slope angle, depth of the weak layer, influence of slope changes), the hydro-mechanical behaviour, input motion (amplitude, duration and frequency content), initial stress state, hydraulic boundary conditions, impedance contrast between soil layer and bedrock, and finally the assumption of continuous vs. discontinuous medium have to be analysed.

Before starting the main computations with complex materials and real accelerograms it is always very useful to make some preliminary computations assuming isotropic homogeneous elasticity in order:

- to evaluate the influence of topography on modulation of the amplitude of seismic motion,
- to determine the seismic wave pattern once diffracted on the geometrical irregularities,
- to verify the minimum dimension of a geometrical disturbance that will be affected by seismic motion
- to verify whether improved simplified methods are sufficient for the analysis or not.

All calculations presented here were performed with the non-linear finite element code GEFDYN (Aubry *et al.* 1985, see also ref. 6).

Geometry of the slope

For the slope geometry it was felt that it would be most rational to focus on a real case along Autostrada A16, in Southern Italy, close to the epicentral zone of the destructive Irpinia earthquake of 1980. Several criteria could be considered for selection of the geometry of the slope to be studied: either an infinite slope or a set of hypothetical slopes, but all with the presence of geometrical irregularities introduced by the motorway and probable presence of filled lands. With an input motion for which the dominant frequency content is less than 5 Hz (the Irpinia event) and assuming a shear wave velocity of 500 m/s the minimum width of the motorway to be taken into account would be larger than current values. A parametric study was carried out with respect to a reference configuration (Fig. 7). The real geometry of the slope (Fig. 8) has been also studied.

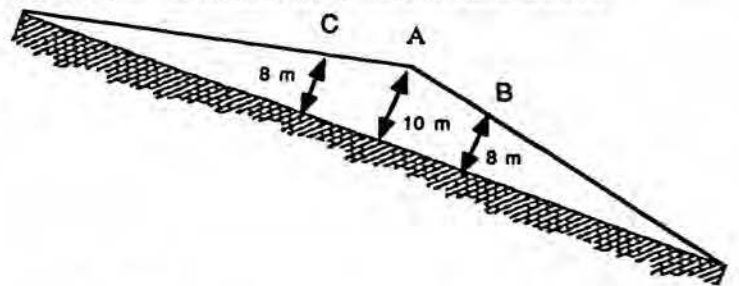


Fig. 7- Reference geometry used for parametric study

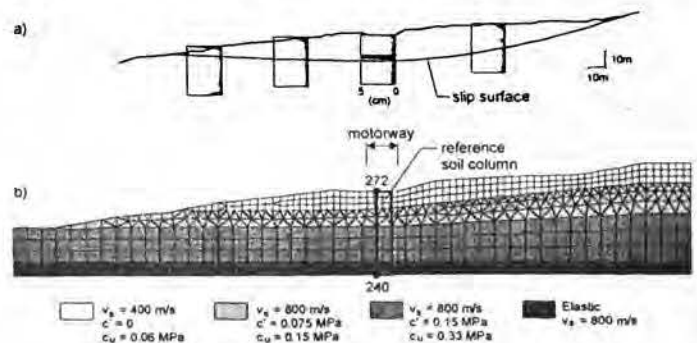


Fig. 8- Real geometry of the soil slope

Input motion

Three input motions have been used through all computations. Two real seismic recordings: a "low" frequency, "long" duration (Irpinia recording) and a "high" frequency "short" duration (Ancona recording), and an analytical wavelet (Ricker) that is commonly used by seismologists. The latter was calibrated on the predominant low-frequency portion of displacement time history of the Irpinia recording that had a magnitude of 6.9. This severe accelerogram (PGA = 0.3 g, significant duration about 20 s) has been recorded at Sturmo, a

few kilometres from the site, on a stiff ground. The input motions considered in different cases studied were the horizontal components of different accelerograms. The vertical components that generally contained relatively higher frequencies were not taken into account because the preliminary computations showed that they had limited influence. Moreover, both real accelerations possess relatively high frequency components. This will naturally increase the computation time for numerical modelling. Therefore, many of the computations were made with the first accelerogram (Irpinia event). The major properties of these input motions are given Table 2.

Input Motion	Max. Hor. Acc. (g)	Duration (s)	Main Freq. (Hz)
Irpinia	0.3	25	0.4, 3, 5, 7
Ancona	0.35	5	7
Ricker wavelet	0.28	5	0.4

Table 2: Main characteristics of accelerograms

Material Properties

A great amount of difficulties are associated with the complex geotechnical behaviour of clayey material in this region. The reference material properties were selected according to the data available for the site and summarised in Table 3.

Material properties	soil slope	bedrock
Shear wave velocity (m/s)	400	∞ / 800
Dilat. wave velocity (m/s) dry	800	∞ /1600
Dilat. wave velocity (m/s) sat.	2040	∞ /4080
Friction Angle ($^{\circ}$)	20	-
Cohesion (MPa)	0.025	-
Dilatancy angle ($^{\circ}$)	10	-
Porosity	0.25	-
Water compressibility (Pa^{-1})	$5.10 \cdot 10^{-10}$	-

Table 3: Material properties

Mass density of the solid phase is 2.7. The angle of shearing resistance is slightly greater than the slope angle and a small cohesion is introduced in order to keep the slope stable under static conditions.

Other calculations, either 1D or 2D (Fig.8), were made in which the mechanical properties vary with the depth (Fig. 9). They correspond to the real slope that lies along the motorway. The slope is made of varicoloured overconsolidated clays, with a weathered upper layer 10-15 m thick

The behaviour of the slope has been modelled either by an elastic-perfectly plastic model with Mohr-Coulomb criterion or by Hujoux (Hujoux 1985) elastoplastic cyclic model. This latter belong to the critical-state type models and allows for a progressive plasticity.

Rigid/deformable bedrock assumption

The rigid bedrock assumption simplifies computational aspects as no absorbing boundaries have to be taken into account. With this assumption the calculation can be done in a moving reference frame that results in a fixed base. Therefore, the computed motion is relative to the prescribed motion at the fixed base. Absolute motion corresponds to the sum of these two motions. In order to verify the influence of an elastic semi-infinite bedrock on seismic results for the studied case, a 2-D calculation was made.

The results in the frequency domain, with totally drained linear isotropic elastic behaviour for soil and bedrock, show that, even for wave velocities in bedrock that are ten times larger than those in soil, the deformability of bedrock still has some influence (Fig. 10).

Synthesis of obtained results

The parametric study has confirmed several well-known observations. The influence of the components of input motion with respect to problem's geometry (frequency content vs. spectral amplification) and the constitutive behaviour of materials (amplitude vs. hardening, duration vs. cyclic behaviour) have been briefly studied. The initial stress state was also identified as other important element in such analyses.

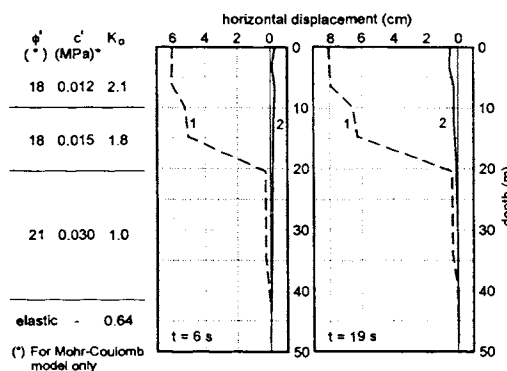


Fig. 9- Displacement profiles of reference soil column (specified in Fig. 8) under drained conditions, at two instants of seismic excitation: 1= Mohr-Coulomb model, 2=Hujoux model. On the left, the assumed effective strength parameters and the earth pressure coefficient.

The elastic-perfectly plastic (Mohr-Coulomb) model shows several aspects, such as the abrupt appearance of irreversible displacement and the concentration of irreversible strain at the interface between bedrock and soil. The results indicate that introduction of deviatoric hardening present in Hujoux model provides:

- o more progressive yielding,
- o plastic damping,
- o more progressive and diffuse deformation,
- o more progressive pore-pressure variation,

If the material is dilatant under the considered stress state, irreversible sliding displacement is larger under dry conditions

than under saturated conditions. This results from the increase of volumetric strain in dilatant materials, which induces a decrease of pore pressure (negative excess pore pressure) and therefore an increase in the mean effective stress.

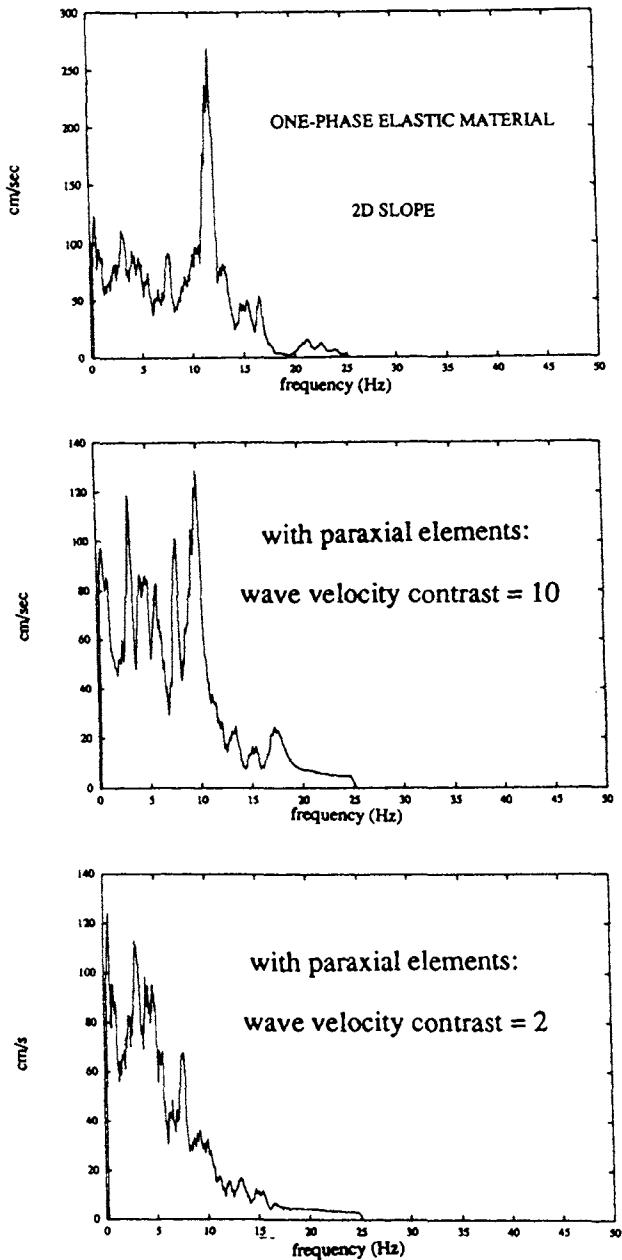


Fig. 10- The influence of the deformability of bedrock Fourier Transform of horizontal acceleration (point "A" Fig.7)

For material properties that lead to contractant behaviour under the considered stress state, the presence of water in the soil generates larger displacement than in dry soil. The increase of pore pressure due to contractance of the material reduces the effective mean stress and may lead to liquefaction. It was thus verified that the water pore pressure plays two main roles: damping due to seepage and mean effective stress decrease causing liquefaction.

The role of input motion was investigated as well (Fig. 11).

For a perfectly plastic model, only the very strong peaks can generate irreversible displacement. Therefore, the amplitude of maximum acceleration and the number of peaks above the elastic limit are the two main factors that determine irreversible displacement. With the Hujieux model, all peaks of the accelerogram can induce irreversible displacement. Therefore, the main factors for irreversible displacement are the number of peaks and their amplitudes. The amplitude of maximum pore pressure is correlated to the amplitude of displacement, and thus depends on the number of peaks and on the type of constitutive model. Higher pore pressure are obtained for Irpinia event (Fig. 12)

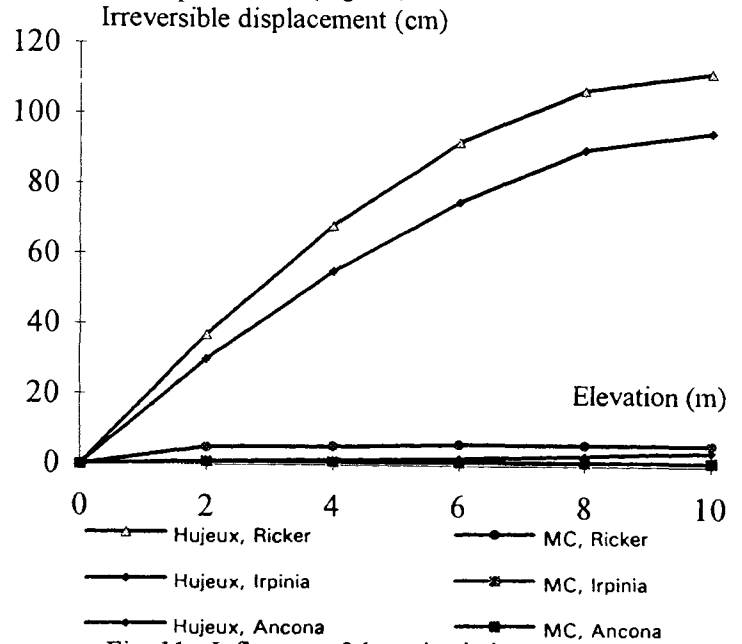


Fig. 11 - Influence of the seismic input motion; Final deformation of slope (1D semi-infinite)

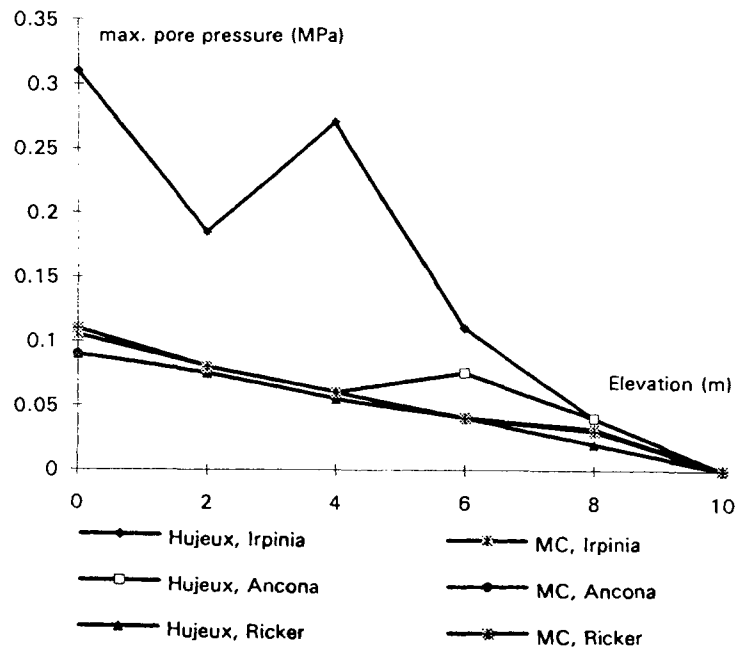


Fig. 12 - Influence of the seismic input motion; Final pore pressure in the slope (1D semi-infinite)

One of the most important factors governing seismic response in soil slopes is the initial stress state. This aspect was only partially studied, as plausible situations are quite numerous and it is very difficult to derive general conclusions from the tests. The computations in saturated case have shown, as expected, that the effect of the initial stress state is mixed with the effect of pore water in soil. In the elastic-perfectly plastic model, the effect of shear-stress/normal-stress ratio depends on the value of cohesion. Its influence is small on displacement curves, but more obvious on pore-pressure curves.

In Fig. 9 the results obtained with Mohr-Coulomb and Hujoux model assumptions and varying properties with respect to the depth are presented. The comparison shows that the elastic perfectly plastic model, with assumed modulus reduction at depth, substantially overpredicts the deformations with respect to the more realistic hardening model. In Fig. 13, the calculated deflections of the soil column are shown at the same instants as in Fig. 9 with different assumptions (1D/2D, one-phase and two-phase analyses). The permeability coefficient are of 10^{-7} and 10^{-6} in horizontal and vertical directions, respectively. The displacements remain small and are not significantly affected by the presence of the fluid phase, so that a drained (one-phase) analysis appears to be adequate for the soil under consideration (Faccioli *et al.* 1994).

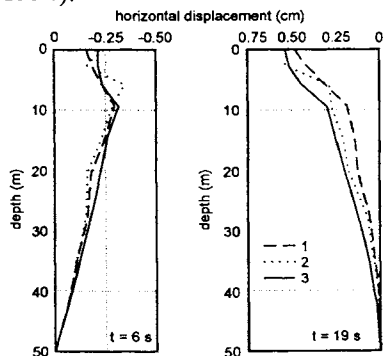


Fig. 13- Displacement profiles of reference soil column (specified in Fig. 8) at two instants of seismic excitation, calculated with Hujoux model, 1=two-phase 1D analysis; 2=one-phase 1D analysis; 3=Two-phase 2D analysis.

It was not always easy to derive conclusions from absolute-displacement time histories. Displacement variations due to geometry or behaviour effects tend to be small compared to the input displacement motion. The Fourier transform of relative displacement in the case of elastoplastic models reveals the well-known (but not trivial) aspect of a shift towards lower frequencies. Such a shift usually is attributed to a possible decrease of elastic moduli with increasing shear-strain amplitude. A further reason can be sought in the fact that the irreversible displacement induced in soil resembles a Heaviside-type function that in the Fourier domain corresponds to a decay function with increasing frequency (Fig. 14).

The influence of geometrical heterogeneity is well known in seismology. The comparison between results obtained

between one- and two-dimensional configurations confirms this point. The eigen frequency for a two-dimensional geometry is higher than that of a one-dimensional assumption, as the latter represents a laterally infinite medium. The kinematics of slope motion are also largely affected when a two-dimensional assumption is made.

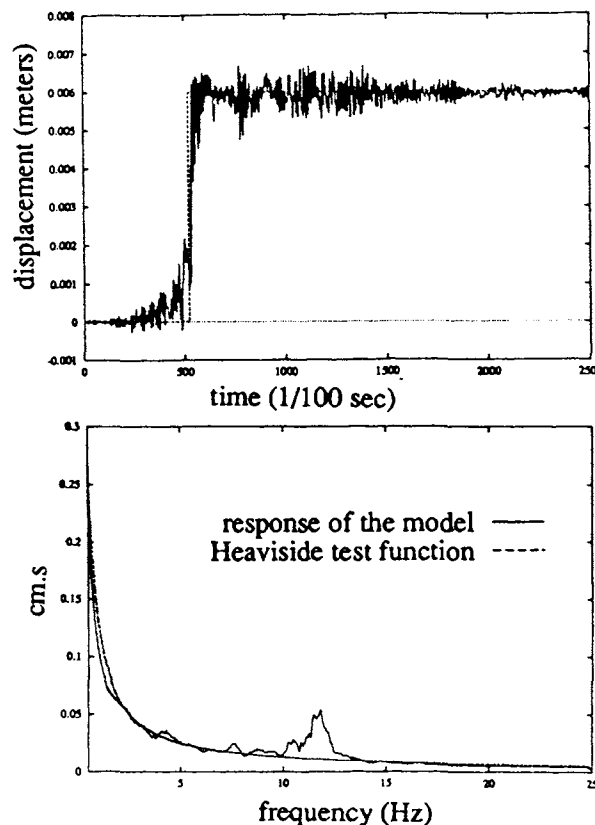


Fig. 14- Relative horizontal displacement time history and its Fourier transform (point "A" Fig. 7) with elastic-perfectly plastic behaviour assumption for soil

CONCLUSION

The work carried out in the framework of a European research project and partly presented herein, points to some interesting indications as regards the assessment of co-seismic permanent displacement of natural slopes. Some improvements to simplified models currently used in practice for the slope stability analysis under seismic loading are proposed. The pore pressure and rate effects have been introduced in the standard rigid-block model.

Another simplified method has proposed that can be considered as being a good balance between complex and simplified methods. Having a very good run-time efficiency and using a reasonable set of parameters it deals with important factors such as dilation and compaction of the soil coupled with the pore pressure increase that are otherwise available only in complex finite element codes.

The interest of using simplified input motions such as Ricker wavelet or Tsang signal is also shown through different computations. For this latter, its amplitude can be determined

according to the expected PGA, its duration can be selected according to the magnitude of the earthquake, and finally, as proposed after the statistical study presented in (Seed *et al.* 1975), the number of cycles of the earthquake can be related to its magnitude.

Although a continuum approach has been chosen with a discretization by finite elements in the vertical direction, it should be pointed out that by selecting one element only, with a lumped mass, the link with a generalised Newmark method with one block is recovered.

Lastly, 2D non linear finite element models for dynamic slope analysis have been discussed in this paper. Even though the lack of seismic field data and a proper choice of parameters associated with the use of complex constitutive models is a severe shortcoming in this respect, they are very useful for a better understanding of the phenomenon and, consequently, for improving the simplified models. Parametric analyses conducted with 1D and 2D models, and one/two-phase material description, for a given site have shown that for a moderate slope angle and no strong lateral heterogeneity, a 1D analysis with rigid bedrock assumption and one-phase behaviour assumption gives satisfactory results with respect to permanent displacements. On the contrary, the kinematics of the motion is totally different and should not be overlooked.

ACKNOWLEDGEMENTS

This work is a part of a European research project that has been partially sponsored by the European Commission under contract n° EPOC CT91-0046 "Analysis and mitigation of earthquake triggered landslide hazard affecting dams, routes and lifelines". C. Battistella and R. Andrighetto from Studio Geotecnico Italiano, O. Ozanam and B. Fauchet from Coyne et Bellier, A. Modaressi from Ecole Centrale de Paris and M. Monkachi from Bureau de Recherches Géologiques et Minières have largely contributed to the topics presented in this paper.

REFERENCES

- [1] Ambraseys N. and Srbulov M., " Earthquake induced displacements of slopes", ESEE Res. Rep. no. 93.18, Dept. of Civil Eng., Imperial College, London, 1993.
- [2] Aubry D., Chouvet D., Modaressi A. and Modaressi H., "GEFDYN 5: logiciel d'analyse du comportement statique et dynamique des sols par éléments finis avec la prise en compte du couplage sol-eau-air", Rapport Scientifique, Ecole Centrale de Paris, (1985).
- [3] Aubry D., Modaressi A. and Modaressi H., A Constitutive Model for Cyclic Behaviour of Interfaces with Variable Dilatancy. *Computers and Geotechnics*, 9, pp 47-58, (1990).
- [4] BRGM "Modélisation des sols en élastoplasticité : définition des paramètres des modèles Hujeux-Cyclade et recherche des valeurs des paramètres pour différents sols" - BRGM report, Feb. 1989.
- [5] Chang C.J., Chen W.F. and Yao J.T.P., "Seismic displacements in slopes by limit analysis", *Journal of Geotechnical Engineering*, ASCE, vol. 110, N. 7, pp.850-874, (1984).
- [6] ECP, COB, EDF, "Manuel Scientifique de GEFDYN", Presse de Coyne et Bellier, (1994).
- [7] Faccioli E., Andrighetto R., Battistella C. and Fontana M., "Modelling the co-seismic displacements of natural slopes in cohesive soils", *Proc. of The second International Conference on Earthquake Resistant Construction and Design*, vol. 3, Berlin, 1994.
- [8] Heiderbrecht A.C., Henderson P., Naumoski N. and Pappin J.W., "Seismic response and design for structures located on soft clay sites" *Can. Geotech. Journal*, 27, pp 330-341,(1990).
- [9] Heiderbrecht A.C., Henderson P., Naumoski N. and Pappin J.W., "Site response effects for structures located on sand sites" *Can. Geotech. Journal*, 27, pp 342-354, (1990).
- [10] Hujeux J.C., "Une loi de comportement pour le chargement cyclique des sols", *Génie Parasismique*, (Ed. Davidovici), Presses Ponts et Chaussées, Paris, pp. 287-302, (1985).
- [11] Newmark N.M., "Effects of earthquakes on dams and embankments", *Geotechnique*, vol. 15, N. 2, pp. 137-150, (1965).
- [12] Sarma S.K., "Stability analysis of embankments and slopes", *Journal of Geotechnical Engineering*, ASCE, vol. 105, N. 12, pp. 1511-1524, (1979).
- [13] Seed H.B., Idriss I.M., Makdisi F. and Benerjee N. "Representation of irregular stress time histories by equivalent uniform stress series in liquefaction analyses" - report No. EERC 75-29, Earthquake Engineering Research Center, University of California, Berkeley, Calif. Oct. 1975.
- [14] Tardieu B., Carrère A., Ozanam O. and Crepel J.M. "New developments in seismic analysis of dams", *Recent Advances in Earthquake Engineering and Structural Dynamics*, Ouest Editions, pp. 547-586, (1992).
- [15] Wilson R.C. and Keefer D.K., "Predicting areal limits of earthquake induced landsliding", in Ziony J.I. (Ed.), *Evaluating Earthquake Hazards in the Los Angeles Region*, U.S. Geological Survey Professional Paper 1360, Washington, pp. 317-345, (1985).